Peer-reviewed version available at Appl. Sci. 2018, 8, 2033; doi:10.3390/app8112033

Article

Form-Finding Analysis on the Rail Cable Shifting System of the Long Span Suspension Bridges

Pan Quan [1,*], Yan Donghuang [2] and Yi Zhuangpeng [3]

School of Civil Engineering, Changsha University of Science & Technology. Changsha 410114, Hunan, China; yandonghuang@126.com (Y.D); yizhuangpeng@163.com (Y.Z)

* Correspondence: panquan605@126.com

Abstract: The determination of the non-loading condition of the rail cable shifting (RCS) system, which consists of main cables, hangers and rail cables, is the premise of the girder erection for the long-span suspension bridges. An analytical form-finding analysis model of shifting system is established according to the basic assumptions of flexible cable structures. Herein, the rail cable is discretized into segmental linear cable elements and the main cable is discretized into segmental catenary elements. Moreover, the calculation and analysis equation of each member and their iterative solutions are derived by taking the elastic elongation of the sling into account. In addition, by taking the girder construction of Aizhai suspension bridge as engineering background, a global scale model of the RCS system is designed and manufactured; also the test system and working conditions are established. The comparison between the test results and analytical results shows the presented analytical method is correct and effective. The process is simplified in the analytical method, and the computational results and precision can satisfy the practical engineering requirements. In addition, the proposed method is suitable to apply to the computation analysis of similar structures.

Keywords: Suspension bridge; Girder construction; RCS process; Form-finding analysis; Model test

1. Introduction

Suspension bridge [1-7] is widely used to cross the long-span barriers in engineering and its mechanical behaviors during construction have attracted the special attention of researchers [8-15]. The girder erection is the key and difficult step for the construction of the long span suspension bridges in mountainous area. To facilitate the transportation and erection, the structural types of girders are often designed as steel trusses. The mature construction methods include the deck crane construction method [16], the cable crane construction method, among others [8-9]. The rail cable shifting (RCS) is a recently invented new method, and it was firstly used in the successful erection of the girder of Aizhai Bridge [17-23]. The erection of the 1000.5m steel truss girder needed only two and a half months [16]. With RCS, the construction period is greatly shortened and the amount of steel used for the steel truss girder is significantly reduced. However, this technology is still in the first time for the practical use, and its large-number promotion requires accumulating more experience. Meanwhile, the understanding and researching of this technology still remains to be further deepened, e.g., whether the analysis process of RCS system can be further simplified, whether the technological process can be further optimized, and whether the equipment and operations can be standardized. All of these restrict the widespread promotion and application of the RCS technology.

In the presented technology, the shifting system is a double-layer flexible suspended cable system that consists of main cables, hangers, saddles and rail cables. With the tension of the track cable and the cable system under stress, the system will undergo relatively obvious deformation, through which the load will be distributed according to the stiffness in the cable system [24-32]. For the long and flexible sling structure, the deviation and elongation will appear in the process of the rail cable tensioning, and the variations should not be ignored. The cable force rail during the tensioning process of the rope sling is unknown, and the implicit solution is needed from the deformation coordination relation of the system. Therefore, all these bring difficulty and complexity

Peer-reviewed version available at Appl. Sci. 2018, 8, 2033; doi:10.3390/app8112033

to the static analysis. During the process of the research and development, the finite element method is used to compute the main cable and the rail cable that are regarded as segmental catenaries, and the computational process is complicated. Moreover, the rail cable has a large pretension force, which is different from the force of the suspension cable segment obtained when only the weight force and sling force on both ends are considered.

In this paper, to simplify the form-finding [33] analysis of the RCS process under the non-loading condition, an analytical method is developed to establish the global mechanical model of the main cable, sling and rail cable and to solve the equation, under the condition that the sling force is unknown. Here, the basic assumptions of the mechanical analysis of flexible cables are introduced and the elastic elongation of the sling is considered. The comparisons among the analytical results, the finite element results and model test results show the presented analytical method is correct and it can be used in the computation and analysis of similar structures.

2. Mechanical characteristics of RCS system under non-loading condition

2.1 Brief introduction to RCS technology

In RCS, the main cable and permanent sling are taken as the supports. A shifting cableway with horizontal pretension force is set below the sling, which is connected with the sling through the saddle. The steel truss girder segments are separately assembled on both sides. A single segment is transported longitudinally via girder transporting vehicles along the girder transporting cableway to the position beneath the permanent sling. The steel truss girder segment is lifted by a cable crane or other hoisting equipment to exit the vehicle. Subsequently, the segments are docked and pin-connected to the sling. A symmetrical construction segment by segment then is performed from the mid-span to the two sides until the full bridge is connected.

The technology allows for the transportation of the entire stiffening girder segment, greatly reduces the aerial work of the girder segment, shortens the construction period, reduces the construction costs, improves the construction quality and safety, and provides an advanced, economical and highly efficient construction for the extra long span suspension bridge in the mountainous area. The difficult problem of construction of the stiffening girder for the extra long span suspension bridge in mountainous areas is solved. It is a major new method for the construction of long span suspension bridges in mountainous areas. Additionally, the construction machines and tools are conventional, and they are easy to operate and control. Moreover, it is also suitable for the girder construction of the half-through and the through arch bridges, thus involves great adaptability and promotion value.

2.2 Mechanical model of RCS system under non-loading condition

During the computation of the conventional suspension bridge construction process, the parameters of main cable are usually solved by the segmental catenary method. The sling force is determined from the completed bridge state backward disassembling to the cable finish state. The internal force, line shape, unstressed cable length and sling length of the unloaded cable can be directly solved through iteration [34]. In the computation and analysis of conventional double-layer cable systems and cable dome structures, the hanger is often considered as rigid handling, or it is assumed with infinite sling stiffness, to ensure that the vertical displacements of the load-bearing cable and the stabilization cable are the same, which is inconsistent with the actual situation. In the finite element analysis of single-layer flexible cables, the two-node straight element, two-node curve element [35], multi-node isoparametric element [36], among others, are usually used. Although there are certain limitations and deviations in the computation accuracy, computational efficiency, and applicable range of each element, the computational results in respective adaptive range can reach high accuracy and can be applied to engineering practice [37].

To simplify the form-finding analysis of the RCS process under the non-loading condition, the analytical method is used to establish the global mechanical model of the main cable, sling and rail cable and to solve the equation, under the condition that the sling force is unknown. The basic

assumptions of the mechanical analysis of flexible cables are introduced and the elastic elongation of the sling is considered. The main cable segment is simulated by a segmental catenary element, and the rail cable segment is simulated by a two-node straight pole element. The analytical results are compared with the finite element results and model test results.

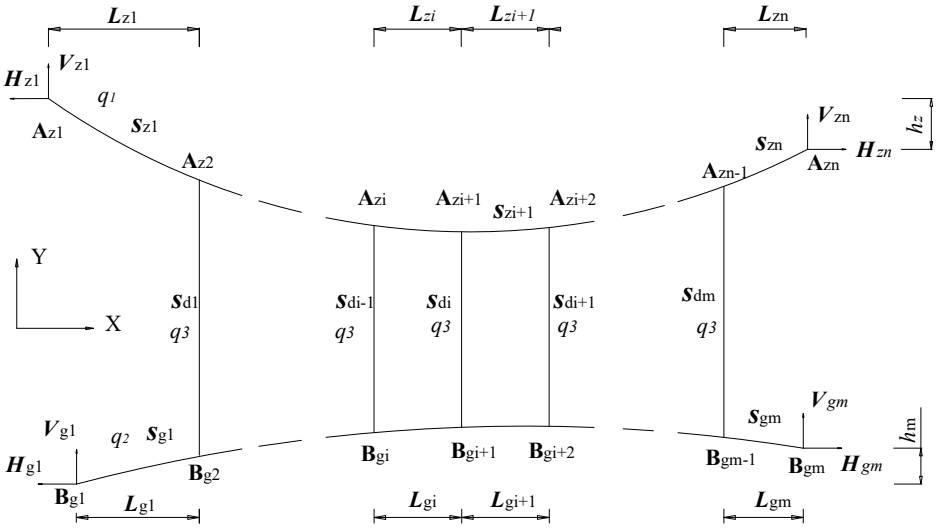

Figure 1. Mechanical analytical model of RCS system under the non-loading condition

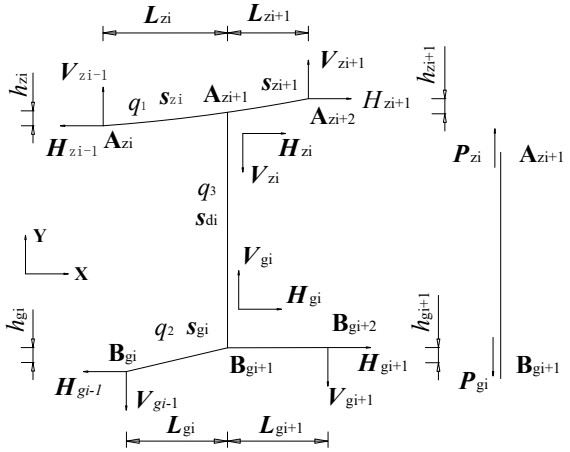

Figure 2. Mechanical discrete model of RCS system under the non-loading condition

The non-loading condition is defined as the status after the erection of the main cable and sling, the installation of the saddle support and the rail cable, and the tensioning of the rail cable are completed. To simplify the computational model for the system under the non-loading condition, the following assumptions are introduced [34]:

1) The flexible cable can only be tensed but not be pressed or bent.
2) The stress-strain of the flexible cable is consistent with Hooke's theorem.
3) The cross-sectional area before deformation is used for the calculation of the tensile stiffness of the main cable, rail cable, and sling before and after stress.
4) The friction between the rail cable and the saddle is ignored, and the sling does not tilt after the rail cable tension is completed.

Then, a mechanical analytical model for the shifting system under the non-loading condition is established as shown in Figure 1, where z represents the main cable, g represents the rail cable, and d represents the sling. To describe the analysis process, an inter-segmental model is extracted for analysis, as shown in Figure 2.

2.2.1 Force analysis of the main cable

As shown in Figure 2, the main cable segment is discretized into two segments: A_{zi}-A_{zi+1} and A_{zi+1}-A_{zi+2} under the non-loading condition. In addition, the corresponding segmental catenary element equations [34] can be established and solved to obtain l_{zi}、h_{zi}、l_{zi+1}、h_{zi+1}、S_{zi}:

$$l_{zi}=\frac{H_{zi}s_{zi}}{E_1A_1}-\frac{H_{zi}}{q_1}\{\ln[V_{zi}+\sqrt{H_{zi}^2+V_{zi}^2}]-\ln[V_{zi}-q_1s_{zi}+\sqrt{H_{zi}^2+(V_{zi}-q_1s_{zi})^2}]\} \tag{1}$$

$$h_{zi}=\frac{q_1s_{zi}^2-2V_{zi}s_{zi}}{2E_1A_1}-\frac{1}{q_1}[\sqrt{H_{zi}^2+V_{zi}^2}]-\sqrt{H_{zi}^2+(V_{zi}-q_1s_{zi})^2}] \tag{2}$$

$$l_{zi}=X_{zi}-X_{zi-1} \tag{3}$$

$$h_{zi}=Y_{zi}-Y_{zi-1} \tag{4}$$

where E_1 and A_1 are elastic modulus and cross-sectional area of the main cable; q_1 is the self-weight per unit length of the main cable; S_{zi} is the segmental cable length after the sling installed to the unloaded cable; i=1~n. Other parameters are shown in Figure 1.

Based on the equilibrium state of A_{zi} node and the sling, two additional equations can be established

$$H_{zi-1}=H_{zi} \tag{5}$$

$$V_{zi}=V_{zi-1}-P_{zi}-q_1s_{zi} \tag{6}$$

where P_{zi} is the force of the sling at A_{zi} node.

2.2.2 Force analysis of rail cable

The diameter, strength grade and type of the rail cable can be determined mainly from its stress level, supporting condition, safety factor, and climbing angle of shifting. As the support of rail cable lies on the saddle connected to the lower anchor point of the sling, the linear sag under non-loading conditions is small. In addition, due to the large pretension force of the rail cable, the influence of its self weight on the line shape of the cable segment is limited. Meanwhile, the assumption that each segment is in line after completion of the rail cable tension is made, which simplifies the force analysis of subsequent shifting process. Therefore, the rail cable can be discretized into the connection of multiple straight poles. A two-node straight pole element is used to simulate the force for the rail cable segment under the non-loading state, and an analytical diagram shown in Figure 3 is obtained. Furthermore, the internal forces of the straight cable segment can be directly obtained by solving the following static equilibrium equations and geometric equations,

$$l_{gi}=\frac{H_{gi-1}}{T_{gi-1}}S_{gi} \tag{7}$$

$$h_{gi}=\frac{V_{gi-1}}{T_{gi-1}}S_{gi} \tag{8}$$

$$\Delta(S_{gi})=\frac{T_{gi}S_{gi}}{E_2A_2} \tag{9}$$

$$T_{gi} = \sqrt{V_{gi}^2 + H_{gi}^2} \tag{10}$$

$$H_{gi-1} = H_{gi} \tag{11}$$

$$S_{gi} = \sqrt{l_{gi}^2 + h_{gi}^2} \tag{12}$$

$$V_{gi} = V_{gi-1} - P_{gi} + q_2 s_{gi} \tag{13}$$

$$l_{gi} = X_{gi} - X_{gi-1} \tag{14}$$

$$h_{gi} = Y_{gi} - Y_{gi-1} \tag{15}$$

where E_2 and A_2 are respectively the elastic modulus and cross-sectional area of the rail cable; q_2 is the self-weight per unit length of the rail cable; S_{gi} is the cable length of the rail cable segment; P_{gi} is the sling force increment; i=1～m. Other parameters are shown in Figure 3.

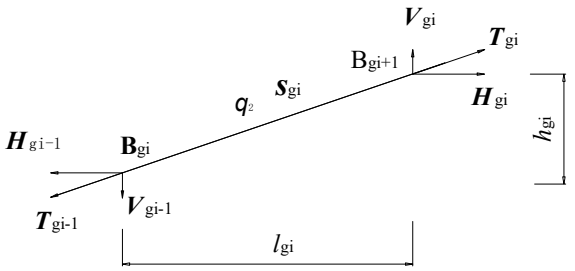

Figure 3. Discretization diagram for two-node straight pole element of the rail cable.

2.2.3. Force analysis of the sling

The force of sling is relatively simple. According to Assumption 4), the tilting of the sling is not taken into account under the non-loading condition. In an actual construction, a secondary adjustment can be applied after the pre-biasing and the tensioning of the rail cable to keep the sling being vertical after the rail cable is tensioned. The coordination relationships between the sling force and the deformation are

$$P_{zi} = P_{gi} + q_3 s_{di} + W\,, \tag{16}$$

$$Y_{zi} - Y_{gi} = \frac{P_{gi}}{E_3 A_3} + S_{di}\,, \tag{17}$$

where W is the constant weight of the saddle; E3 and A3 are the elastic modulus and cross-sectional area of the sling, respectively; q_3 is the self-weight per unit length of the sling; and S_{di} is the unstressed cable length of the sling. Other parameters are shown in Figure 1.

2.3 Solution analysis of the system

Before the tensioning of the rail cable, the longitudinal position l_g of the two anchorage points, the pretension force T_{g0} and the unstressed cable length of the sling are known. After the installation of the sling, the cable force, line shape, cable tower distance l_z and the height difference

Peer-reviewed version available at Appl. Sci. 2018, 8, 2033; doi:10.3390/app8112033

h_z can be computed according to actual conditions. On this basis, other unknown variables can be solved by an iterative method. The iterative scheme is shown below:

1) Assume the horizontal force H_{g0} and the elevation h_{g0} at the left support of the rail cable; the horizontal force H_{z0} at the left support of the main cable, and the increment of the cable force of the sling P_{g1};

2) Obtain H_{gi}, H_{zi} from Eqs. (4) and (11);

3) Substitute them into Eqs. (10), (13), (7), (8) and (9), V_{g0}, V_{g1}, l_{g1}, h_{g1} and T_{g1} are obtained;

4) From the coordination relation of deformation, Y_{g1}, Y_{z1} and h_{z1} are obtained by combing with Eqs. (15), (17), and (4), respectively;

5) Substitute Y_{g1}, Y_{z1} and h_{z1} into Eqs. (1) and (2), V_{z0} and l_{z1} can be obtained;

6) Substitute V_{z0} and l_{z1} into Eqs. (16), (6) and (13), P_{z1}, V_{z1} and V_{g2} can be obtained;

7) Substitute P_{z1}, V_{z1} and V_{g2} the results of step 6) into Eqs. (2), (1), (10), (7) and (8), h_{z2}, l_{z2}, T_{g2}, l_{g2} and h_{g2} can be acquired respectively;

8) Substitute them into Eqs. (4), (15), and (17), Y_{z2}, Y_{g2}, and P_{g2} are obtained;

9)Follow the similar iterative manner, all l_{gi}, l_{zi}, h_{gi}, and h_{zi} are obtained;

10) Check convergence conditions $\Delta_{z1} = \left|\sum_{i=1}^{n} l_{zi}\right| - l_z \le \varepsilon$ (ε=1×10^{-6} is the given error limit), $\Delta_{z2} = \left|\sum_{i=1}^{n} h_{zi}\right| - h_z \le \varepsilon$, $\Delta_{g1} = \left|\sum_{i=1}^{m} l_{gi}\right| - l_g \le \varepsilon$, and $\Delta_{g2} = \left|\sum_{i=1}^{m} h_{gi}\right| - h_{g0} \le \varepsilon$. If they are satisfied, go to the next step. If not, letting $H_{z0} = H_{z0} + \frac{\Delta_{z1}}{DH_z}$, $P_{g1} = P_{g1} + \frac{\Delta_{z2}}{DP_g}$, $H_{g0} = H_{g0} + \frac{\Delta_{g1}}{DH_g}$, and $h_{g0} = h_{g0} + \frac{\Delta_{g2}}{Dh_g}$, and return to step 1), iteratively recalculating, where DH_z, DP_g, DH_g and Dh_g are respectively the first derivatives of H_{z0}, P_{g1}, H_{g0}, and h_{g0} [38].

Then, all the sling forces and the coordinates of each node are determined. Substituting the results into Eqs. (9), (12), the unstressed cable length and the anchorage point elevation of the rail cable can be obtained.

3. Global Model Test of Moving Girder by Rail Cable

The rail cable launching method is the first used in the Aizhai suspension bridge to realize the horizontal movement of the girder segment. The horizontal cableway utilizes eight relatively independent 60-ZZZ-1570 type sealed steel wire ropes as rail cable. One side of the rail cable is anchored by the OVM-CPS shear force dispersing type rock anchor system, while the other side is anchored in balance weight. The pretension force of a single rail cable is 105t. The global laboratory experimental model was designed and manufactured with a geometrical reduced-scale ratio of 1:33. The span size of the main cable of the model is 7.333+35.636+3.515 m, its center spacing is 818 mm, and the longitudinal spacing of the sling is 439.4 mm, as shown in Figure 4.

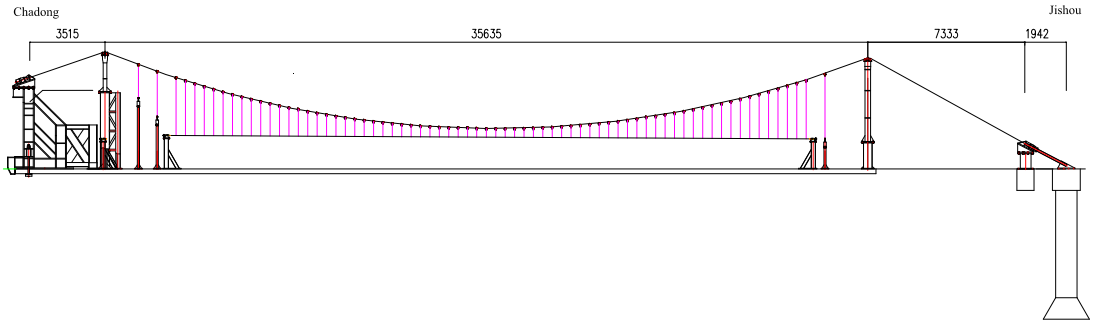

Figure 4. The global model of the Aizhai suspension bridge (unit: mm).

The test model [39] mainly consists of 2 anchorage systems, 2 main cables, 68 pairs of slings and cable clamps, 3 pairs of rock anchor cables, 2 cable towers and cable towers buttresses, rail cables, rail tensioning devices, and test systems. According to the principle of stress equivalence and similar axial stiffness, the parameters of the rail cable are designed. Four φ2.5mm high-strength galvanized steel wire ropes are selected to replace rail cables. The rail cable tensioning device is designed to adjust the relative movement of the screws and nuts to achieve the tensioning of rail cables. A pressure sensor is used to monitor the changes of their cable forces in real time.

On the basis of the global model test design, the finite element software MIDAS Civil is used to establish the full bridge numerical modeling on the initial state. In the test process, the no-load stage of the cable is ensured to be consistent with the finite element analysis model by adjusting the no-load stage of the test model. After the cable clamps, slings and saddles are installed, four rail cables are tensioned and the slings are in vertical working condition. Then, the main cable force and line shape, rock anchor cable force, rail cable line shape and sling cable under the tension working condition are tested to find out the changes.

4. Testing Results of Model Test

After the completion of the rail cable tensioning, the finite element results, experimental results and the analytical results are compared. The responses of several representative locations are compared in Table 1, and the cable forces at the anchor points of the main cable are shown in Table 2.

Table 1 Effects of the working condition of rail cable tensioning on the systematical line shape.

Items	main cable displacement at mid-span		main cable displacement at 1/4 span on Jishou side		main cable displacement at 1/4 span on Chadong side	
	X direction /mm	Y direction /mm	X direction /mm	Y direction /mm	X direction /mm	Y direction /mm
Finite element solution	1.4	28.6	-0.6	9.0	3.6	7.7
Model test measured value	1.5	27.5	-0.5	8.9	3.5	7.5
Analytical Calculation results	1.6	26.3	-0.6	8.7	3.7	7.2
Deviation of the finite element solution from the measured value/%	6.67	4.00	20.00	1.12	2.86	2.67
Deviation of the analytical method from the measured value /%	6.67	4.36	20.00	2.25	5.71	4.00

Note: The measured value is the average of the upstream and downstream measuring points. The value is negative when the X-direction measuring point moves to Jishou side and when the Y-direction measuring point moves to the upstream, and vice versa.

Table 2 Effects of the working condition of rail cable tensioning on the force of main cable.

Main cable force at the anchor point	Finite element solution /kN	Model test measured value /kN	Analytical results /kN	Deviation of the finite element solution from the measured value /%	Deviation of the analytical method from the measured value /%
Jishou side	61.7	59.9	61.3	3.01	2.34
Chadong side	58.5	57.1	58.2	2.45	1.93

From Table 1, it can be seen that the deviation of the results gained by the analytical method from measured values and finite element values in the Y direction is small, the maximum deviation are 4.36% and 4.00%, respectively. It is shown in Table 2 that the deviation of the main cable force at the anchorage point is small with its maximum of 2.34%. The deviation of the main cable displacement of the mid-span, the 1/4 span on Jishou side and the 1/4 span on Chadong side in X-direction is relatively large, which is mainly due to the small deformation value in the X direction and the test system accuracy. The comparison between the test results and the analytical results shows that the presented method can be applied to the form-finding computational analysis of the RCS system under the non-loading condition, which can simplify the analysis of the RCS system. The deviations of the simplified analytical results with the finite element results and model test results are less than 5%, which validates that the proposed method can be used in engineering practice.

5. Conclusions

With the application of the basic assumptions of flexible cables, the analytical form-finding analysis model of the rail cable shifting system is proposed. The rail cable and main cable are seen as segmental linear cable elements and catenary elements respectively. The elastic elongation of the sling is considered to determine the analytical equation of each member and the iterative solutions. Besides the experimental data of the girder construction of the Aizhai suspension bridge, the compared results verify the accuracy and effectiveness of the presented method. The main conclusions are drawn as follow.

(1) The global mechanical analytical model for the main cable, slings, and rail cables of the RCS system under the non-loading condition is established through the theoretical derivation. The equilibrium equation established from the position after structural deformation can be used to perform the geometrical nonlinear analysis of the structural large deformation. The simplified calculation and analysis process of the RCS system achieve sufficient accuracy, which thus can be applied in engineering.

(2) Under the condition that the initial geometric state of the RCS system is unknown, the true internal force and geometry of the rail cable can be iteratively computed by assuming the initial force or configuration of the rail cable.

(3) The designed rail cable tensioning and testing device basically meet requirements of the model test. The measured results of the main cable line shape and main cable force in the model test are in good agreement with the theoretical results.

Author Contributions: Pan quan: Conceptualization, Data curation, Formal analysis; Yan donghuang: Funding acquisition; Yi zhuangpeng: software, Writing – review & editing.

Funding: The National Natural Science Foundation of China (Grant no.51678069); the Key Discipline Fund Project of Civil Engineering of Changsha University of Sciences and Technology (Grant no. 15KB03).

Conflicts of Interest: The authors declared that they have no conflicts of interest to this work.

References

1. Yuwang Xu, Ole Øiseth, Torgeir Moan, Time domain simulations of wind- and wave-induced load effects on a three-span suspension bridge with two floating pylons, Marine Structures, 2018, 58: 434-452
2. Toshio Miyata, Isao Okauchi, Naruhito Shiraishi, Nobuyuki Narita, Toshihiko Narahira, Preliminary design considerations for wind effects on a very long-span suspension bridge, Journal of Wind Engineering and Industrial Aerodynamics, 1988, 29(1-3): 379-388
3. D. M. Siringoringo, Y. Fujino, Observed Along wind Vibration of a Suspension Bridge Tower and Girder, Procedia Engineering, 2011, 14: 2358-2365
4. Hao Wang, Ai-qun Li, Jian Li, Progressive finite element model calibration of a long-span suspension bridge based on ambient vibration and static measurements, Engineering Structures, 2010, 32(9): 2546-2556
5. Ole Øiseth, Anders Rönnquist, Ragnar Sigbjörnsson, Simplified prediction of wind-induced response and stability limit of slender long-span suspension bridges, based on modified quasi-steady theory: A case study, Journal of Wind Engineering and Industrial Aerodynamics, 2010, 98(12): 730-741
6. H. Erdoğan, E. Gülal, The application of time series analysis to describe the dynamic movements of suspension bridges, Nonlinear Analysis: Real World Applications, 2009, 10(2): 910-927
7. Toshio Miyata, Hiroki Matsumoto, Masahiko Yasuda, Circumstances of wind-resistant design examinations for very long suspension bridge, Journal of Wind Engineering and Industrial Aerodynamics, 1992, 42(1-3): 1371-1382
8. Yuhshi Fukumoto, Steel bridge construction in Japan, Journal of Constructional Steel Research, 1989, 13(2–3): 259-267
9. Ho-Kyung Kim, Myeong-Jae Lee, Sung-Pil Chang, Determination of hanger installation procedure for a self-anchored suspension bridge, Engineering Structures, 2006, 28(7): 959-976
10. Shengli Li, Yonghui An, Chaoqun Wang, Dongwei Wang, Experimental and numerical studies on galloping of the flat-topped main cables for the long span suspension bridge during construction. Journal of Wind Engineering and Industrial Aerodynamics, 2017, 163: 24-32
11. J. M. Ko, S. D. Xue, Y. L. Xu, Modal analysis of suspension bridge deck units in erection stage, Engineering Structures, 1998, 20(12): 1102-1112
12. Süleyman Adanur, Murat Günaydin, Ahmet Can Altunişik, Barış Sevim, Construction stage analysis of Humber Suspension Bridge, Applied Mathematical Modelling, 2012, 36(11): 5492-5505
13. G. Diana, Y. Yamasaki, A. Larsen, D. Rocchi, M. Portentoso, Construction stages of the long span suspension Izmit Bay Bridge: Wind tunnel test assessment, Journal of Wind Engineering and Industrial Aerodynamics, 2013, 123, Part B, 300-310
14. Yongxin Yang, Lei Zhang, Quanshun Ding, Yaojun Ge, Flutter performance and improvement for a suspension bridge with central-slotted box girder during erection. Journal of Wind Engineering and Industrial Aerodynamics, 2018, 179: 118-124
15. Taejun Cho, Tae Soo Kim, Probabilistic risk assessment for the construction phases of a bridge construction based on finite element analysis, Finite Elements in Analysis and Design, 2008, 44(6-7): 383-400
16. Liu G, Peng Y, Zhou P, et al. Research on Erection Methods of Steel Stiffening Truss Girder for Baling River Bridge. Journal of Highway and Transportation Research and Development (English Edition), 2010, 4(2): 50-56.
17. Qi-Hua Zhang, Yu-Jie Li, Mei-Wan Yu, et al. Study of the rock foundation stability of the Aizhai suspension bridge over a deep canyon area in China, Engineering Geology, 2015, 198: 65-77.
18. Haojun Tang, Yongle Li, Yunfei Wang, et al. Aerodynamic optimization for flutter performance of steel truss stiffening girder at large angles of attack, Journal of Wind Engineering and Industrial Aerodynamics, 2017, 168: 260-270.

19. Guoqing Huang, Xu Cheng, Liuliu Peng, et al, Aerodynamic shape of transition curve for truncated mountainous terrain model in wind field simulation, Journal of Wind Engineering and Industrial Aerodynamics, 2018, 178, 80-90,
20. Zhi Fang, Kuangyi Zhang, Bing Tu, Experimental investigation of a bond-type anchorage system for multiple FRP tendons, Engineering Structures, 2013, 57: 364-373,
21. Yu S, Ou J. Structural health monitoring and model updating of Aizhai suspension bridge. Journal of Aerospace Engineering, 2016, 30(2): B4016009.
22. Jianhua H, Ruili S. Technical innovations of the Aizhai Bridge in China. Journal of Bridge Engineering, 2014, 19(9): 04014028.
23. Han Y, Li K, He X, et al. Stress analysis of a long-span steel-truss suspension bridge under combined action of random traffic and wind loads. Journal of Aerospace Engineering, 2018, 31(3): 04018021.
24. SHEN R, YAN Y, TANG M, et al. Design and Installation of Full-Scale Sectional Model for Testing of Rail Cable Launching Method. Bridge Construction, 2013, 1: 005. (in Chinese).
25. Huang, J.Z., Li, D.S., Li, H.N., Song, G.B. and Liang, Y., 2018. Damage identification of a large cable-stayed bridge with novel cointegrated Kalman filter method under changing environments. Structural Control and Health Monitoring, 25(5), p.e2152.
26. Zhou, P., Liu, M., Li, H. and Song, G., 2018. Experimental investigations on seismic control of cable-stayed bridges using shape memory alloy self-centering dampers. Structural Control and Health Monitoring, 25(7), p.e2180.
27. M. Liu, G. Song, and H. Li, "Non-model based semi-active vibration suppression of stay cables using Magneto-Rheological (MR) fluid damper," Smart Materials and Structures, Vol.16, pp. 1447-1452, August, 2007.
28. M. Liu, V. Sethi, G. Song, & H. Li, 2008. Investigation of locking force for stay cable vibration control using magnetorheological fluid damper. Journal of Vibration and Acoustics, 130(5), 054504.
29. Y. L. Xu, J. M. Ko, Z. Yu. Modal analysis of tower-cable system of Tsing Ma long suspension bridge, Engineering Structures, 1997, 19(10): 857-867
30. Xuwen An, P. D. Gosling, Xiaoyi Zhou, Analytical structural reliability analysis of a suspended cable, Structural Safety, 2016, 58: 20-30
31. Ming-Hui Huang, David P. Thambiratnam, Nimal J. Perera, Vibration characteristics of shallow suspension bridge with pre-tensioned cables, Engineering Structures, 2005, 27(8): 1220-1233
32. Yuan Sun, Hong-Ping Zhu, Dong Xu, A specific rod model based efficient analysis and design of hanger installation for self-anchored suspension bridges with 3D curved cables, Engineering Structures, 2016, 110: 184-208
33. Huang Y H, Fu J Y, Gan Q, et al. New method for identifying internal forces of hangers based on form-finding theory of suspension cable. Journal of Bridge Engineering, 2017, 22(11): 04017096.
34. ZHANG Li, ZHANG Qilin, DING Peimin. Initial equilibrium and geometry zero state solution methods for cable structures . Journal of Tongji University,2000, 28(1):9-13. (in Chinese).
35. YANG Menggang, CHEN Zhenqing.The non-linear finite element analysis for two-node catenary element of cable structure based on UL formulation. China Civil engineering, 2003, 36(8): 63-68, (in Chinese).
36. TANG Jianmin,SHEN Zuyan,QIAN Ruojun. Finite element method with curved cable element for the nonlinear analysis of cable domes. Journal of TONGJI University,1996,24(1):6-10, (in Chinese).
37. SHEN Ruili , ZHANG Dingsheng, SHEN Zijun .The mechanical properties of the suspension cable structure in aerobus transit system, China Civil engineering ,2004,37(4)：13-18, (in Chinese).
38. BAO Lixin . Analysis of aerobus transportation system static and dynamic behavior, Chengdu：College of Civil Engineering，Southwest Jiaotong University, 2007: 21-46, (in Chinese).
39. FENG Jian .The Research on Scale Model Design of Aizhai suspension bridge. Changsha: School of Civil Engineering and architecture, Changsha University of Science and Technology, 2010: 23-45, (in Chinese).